Cardiovascular Research (2013) **99**, 452–460
doi:10.1093/cvr/cvt132

Neural crest cells are required for correct positioning of the developing outflow cushions and pattern the arterial valve leaflets

Helen M. Phillips, Pavithra Mahendran, Esha Singh, Robert H. Anderson, Bill Chaudhry, and Deborah J. Henderson*

Institute of Genetic Medicine, Newcastle University, Newcastle upon Tyne NE1 3BZ, UK

Received 18 December 2012; revised 15 April 2013; accepted 7 May 2013; online publish-ahead-of-print 30 May 2013

Time for primary review: 58 days

Aims Anomalies of the arterial valves, principally bicuspid aortic valve (BAV), are the most common congenital anomalies. The cellular mechanisms that underlie arterial valve development are poorly understood. While it is known that the valve leaflets derive from the outflow cushions, which are populated by cells derived from the endothelium and neural crest cells (NCCs), the mechanism by which these cushions are sculpted to form the leaflets of the arterial valves remains unresolved. We set out to investigate how NCCs participate in arterial valve formation, reasoning that disrupting NCC within the developing outflow cushions would result in arterial valve anomalies, in the process elucidating the normal mechanism of arterial valve leaflet formation.

Methods and results By disrupting Rho kinase signalling specifically in NCC using transgenic mice and primary cultures, we show that NCC condensation within the cardiac jelly is required for correct positioning of the outflow cushions. Moreover, we show that this process is essential for normal patterning of the arterial valve leaflets with disruption leading to a spectrum of valve leaflet patterning anomalies, abnormal positioning of the orifices of the coronary arteries, and abnormalities of the arterial wall.

Conclusion NCCs are required at earlier stages of arterial valve development than previously recognized, playing essential roles in positioning the cushions, and patterning the valve leaflets. Abnormalities in the process of NCC condensation at early stages of outflow cushion formation may provide a common mechanism underlying BAV, and also explain the link with arterial wall anomalies and outflow malalignment defects.

Keywords Congenital heart disease • Bicuspid aortic valve • Neural crest cells • Mouse heart development

1. Introduction

Bicuspid aortic valve (BAV) is the most common congenital abnormality occurring in 1–2% of the population.[1] It frequently occurs in conjunction with other outflow malformations, most commonly coarctation of the aorta, persistent patency of the ductus arteriosus, and ventricular septal defects (VSDs).[1] Although usually asymptomatic at birth, BAV predisposes to valve disease in later life and is associated with increased risk of developing thoracic aortic aneurysms and dissections.[2] Abnormalities in neural crest cells (NCCs) have been suggested to link these pathologies.[3,4] NCCs are necessary for outflow tract septation[5] and are also associated with alignment defects such as double outlet right ventricle (DORV) and VSDs.[6,7] More recent studies have suggested that NCCs are also important for the formation and/or remodelling of the arterial (semilunar) valves,[4,8] although the precise role of NCCs in arterial valvulogenesis remains unclear.

The two Rho kinase isoforms (Rock 1 and 2) are highly conserved serine/threonine kinases[9] with similar expression patterns and apparent roles during embryonic development.[10] Chemical inhibition and genetic studies have shown Rock to be involved in fundamental cellular processes such as contraction, adhesion, migration, apoptosis, and proliferation.[9] Knockout of the two Rock isoforms independently does not result in cardiac defects.[10,11] However, disruption of ROCK signalling in chick embryos using the specific chemical inhibitor Y27632 results in a range

* Corresponding author. Tel: +44 1912418644; fax: +44 1912418666. Email: deborah.henderson@ncl.ac.uk

of cardiac anomalies.[12] Other studies in chicken have suggested that Rock regulates NCC delamination from the neural tube.[13] We thus reasoned that blocking Rock function may be a useful tool for investigating the importance of NCC in formation of the arterial valves.

2. Methods

2.1 Mice and embryos

Rock dominant-negative (*RockDN*) mice[14] (BRC no. 01294) were intercrossed with the *Wnt1-cre* line as well as the *ROSA 26R* or *ROSA-EYFP* reporters lines. *Tie2-cre* mice were also utilized. For references for all of the mouse lines used in this study, see the Supplementary material online, Methods. This work was approved by the Newcastle University Ethical Review Committee and conformed to Directive 2010/63/EU of the European Parliament.

2.2 Quantitative real-time PCR

The relative quantities of the *CAT* gene cassette were measured from E11.5 outflow tracts by quantitative real-time PCR, as described in Phillips *et al.*[15] Primer sequences were as described in Phillips *et al.*[15]

2.3 Histology and immunohistochemistry

Standard protocols were used for H&E, elastin, and βgal staining of paraformaldehyde fixed embryos. Immunohistochemistry was performed on paraffin sections, cryosections, or NCCs on coverslips. Details can be found in the Supplementary material online, Methods. For comparisons between different levels of the outflow tract in controls and mutants, distance was calculated by counting serial sections. Statistical tests used are described in the Supplementary material online, Methods.

2.4 Neural crest cell cultures

Neural folds from the hindbrain of embryonic day (E)8.5-E9.5 embryos[16] (control or *RockDN*$^{+}$; *Wnt1-cre*$^{+}$ embryos) were placed on fibronectin-coated coverslips and maintained for 2 days, with 10 μm Y27632 (Sigma) added on Days 2–4.

2.5 Three-dimensional reconstruction

Three-dimensional (3D) reconstructions were carried out from serially sectioned embryos using Amira 4.0 according to standard protocols.[17]

3. Results

3.1 Rock signalling is required for normal outflow development

To investigate the potential roles for ROCK signalling in the developing outflow tract, we carried out immunohistochemistry for Rock1 and Rock2 during key stages of outflow development between E9.5-E11.5. Whereas Rock2 was expressed at the low level at these stages, Rock1 localized to both the outflow myocardium and to cells within the outflow cushions that were confirmed as NCC (*Figure 1A–D* and Supplementary material online, *Figure S1*). To investigate the importance of Rock signalling in NCC contributing to the developing outflow region, we utilized the *RockDN* mouse[14] together with the *Wnt1-cre* line. This approach allowed the simultaneous blockade of both Rock1 and Rock2 signalling; this was important as loss of either isoform in isolation does not result in cardiac defects.[10] Efficient activation of the DN cassette was confirmed in *RockDN;Wnt1-cre* outflow tracts (Supplementary material online, *Figure S2*).

3.2 Disruption of NCC results in bicuspid arterial valves and associated malformations

Analysis of *RockDN;Wnt1-cre* mutants and control littermates at E12.5–E15.5 revealed abnormalities in both the aortic and pulmonary valves in 27/31 mutants (87%; *Table 1*), but no controls. In 12/31 mutants (39%), these were found together with DORV and doubly committed VSDs (*Table 1*); the remainder of the valve defects occurred in the context of an otherwise normal heart.

Figure 1E illustrates how the leaflets form from the outflow cushions in the normal heart[18] and clarifies the nomenclature used here. NCCs were abundant in the outflow cushions of control hearts at E10.5 and E11.5 (*Figure 1F* and *G*). By E12.5, distinct valve leaflets were apparent. At this stage, all three aortic valve leaflets had contributions from NCC, although the contribution was reduced in the non-coronary compared with the coronary leaflets (*Figure 1H* and *N*). More obviously, only the right and left leaflets of the pulmonary valve contained NCC-derived cells (4/4); the anterior leaflet, derived from the pulmonary intercalated cushion, contained very few NCC (*Figure 1I* and *N*). This pattern was maintained at E15.5 (*Figure 1J* and *K*) and NCCs were also abundant in the arterial valve leaflets at postnatal day 21 (Supplementary material online, *Figure S3*). *Tie2-cre*-expressing endothelium cells (EDCs) were found within the core of the aortic and pulmonary valve leaflets at E12.5 (*Figure 1L*, *M*, and *O*) and were also maintained at postnatal day 21 (Supplementary material online, *Figure S3*). Thus, EDCs and NCCs were discretely localized, with the latter contributing differentially to the leaflets of the aortic and pulmonary valves.

Examination of *RockDN;Wnt1-cre* mutants at E15.5 revealed a variety of arterial valve anomalies including bicuspid (13/31) and quadricuspid (3/31) leaflets, most commonly affecting the aortic valve, frequently in the presence of dysplasia (*Table 1*). Valve leaflets were abnormally positioned within the turret of the arterial root and varied in size (*Figure 2*). There was no association between bicuspid valves and the presence of DORV ($X^2 = 0.35$, $P > 0.5$; Supplementary material online, *Table S1*); thus, BAV was not secondary to these more severe outflow malformations. The phenotype of the bicuspid valves varied, although it could be explained on the basis of fusion between the right coronary and non-coronary leaflet, or the absence of the non-coronary leaflet (*Figure 2A–H*). In the case of the quadricuspid valves, the leaflets manifested as two large and two small leaflets (Supplementary material online, *Figure S4*). Ectopic origin of the left coronary artery from a dorsal position was observed in 24/31 of the *RockDN;Wnt1-cre* mutants (*Figure 2I* and *J*). No control embryos ($n = 30$) exhibited coronary arteries arising from this position. Three coronary arteries were also seen in one mutant (Supplementary material online, *Figure S5*). Although the mutant offspring die in the perinatal period precluding examination of the adult valves, we have observed valve anomalies in newborn pups, suggesting the anomalies persist (data not shown).

Immunohistochemistry for αSMA revealed abnormalities in the arrangement of the smooth muscle cell (SMC) layers within the NCC-rich regions of the aortic tree, including the aortic root and the walls of the ascending aorta and pulmonary trunk, in *RockDN;Wnt1-cre* embryos at E15.5. In contrast, there was only mild disruption of the elastic laminae as shown by Miller's elastin staining (Supplementary material online, *Figure S6*).

3.3 Abnormal NCC behaviour in the outflow cushions in *RockDN;Wnt1-cre* embryos

We next investigated how disrupting Rock affected NCC within the outflow region. At E8.5-E10.5 when NCC migrated towards the distal outflow tract, the overall distribution of NCC in the *RockDN;Wnt1-cre* embryos was similar to controls (*Figure 3A* and *B* and Supplementary material online, *Figure S7*). However, as the NCC migrated into the distal outflow cushions at E10.5, the distribution of NCC appeared patchy

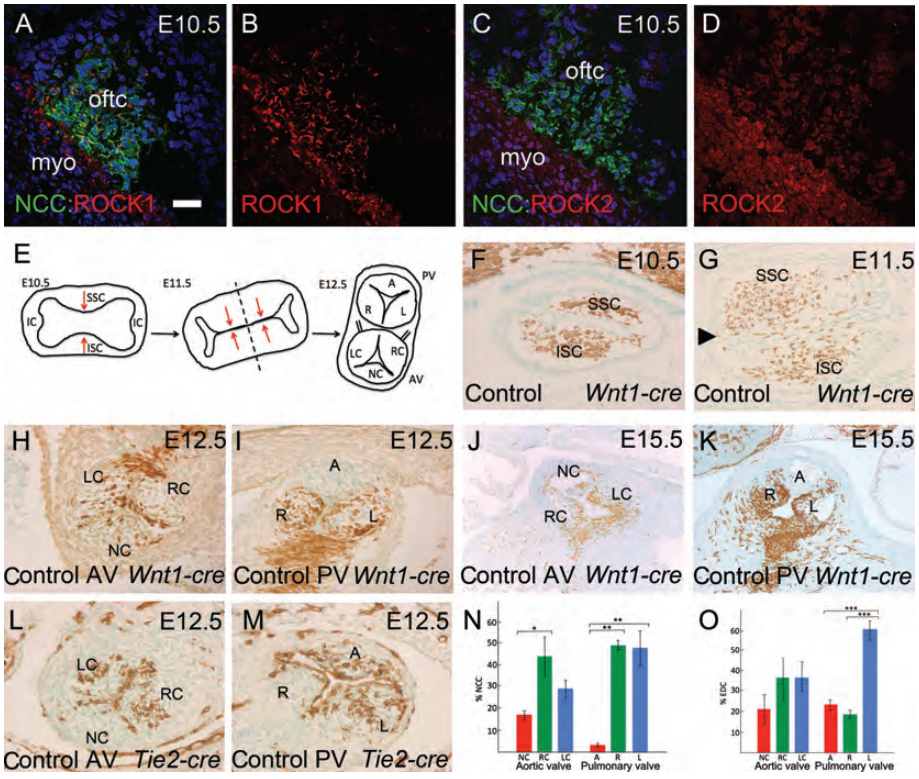

Figure 1 Cellular contributions to the developing arterial valves in the normal mouse heart. *Wnt1-cre* and *Tie2-cre* mice were used together with *Rosa-EYFP* to label NCC and EDC, respectively. NCCs are stained green in (*A*–*D*) and brown in (*F*–*K*). EDCs are stained brown in (*L* and *M*). All sections are coronal, except (*K*), which is transverse. (*A* and *B*) Rock1 (red) is expressed by NCCs in the outflow cushions at E10.5. Dual-stained cells are yellow. (*C* and *D*) In contrast, Rock2 (red) is expressed at lower level and is restricted to the outflow myocardium. (*E*) Model showing how the outflow cushions form the arterial valve leaflets. The dotted line shows the plane of separation between the two forming vessels. (*F*) NCCs colonize the cardiac jelly at E10.5, localized to superior and inferior clusters in the mid-region of the outflow tract. (*G*) By E11.5, the main outflow cushions have formed and are fusing to separate the aortic and pulmonary channels. The aortic intercalated leaflet (arrowhead) can also be seen in this section. (*H*–*K*) At E12.5 and E15.5, NCCs are found in all three leaflets of the aortic valve, but only the right and left leaflets of the pulmonary valve. (*L* and *M*) EDCs are found in all three leaflets of both the arterial valves at E12.5. (*N* and *O*) Quantification of the numbers of NCCs and EDCs in each leaflet of the arterial valves. A, anterior; AV, aortic valve; IC, intercalated cushions; ISC, inferior septal cushion; L, left; LC, left coronary; myo, myocardium; NC, non-coronary; oftc, outflow tract cushion; PV, pulmonary valve; R, right; RC, right coronary; SSC, superior septal cushion. Scale bar (*A*–*D*) = 50 μm, (*F*–*I*, *L*, and *M*) = 75 μm, (*J* and *K*) = 150 μm. *$P < 0.05$; **$P < 0.01$; ***$P < 0.005$.

in the mutant embryos, with aggregation of some, but wide separation of other NCC groups (*Figure 3C–F*). By E11.5, the NCCs were aligning and elongating as they condensed within the outflow tract cushions of control embryos. This condensation process was disrupted in the mutant embryos, with some clustering, but also large gaps between groups of NCCs (*Figure 3G* and *H*). NCCs were abnormally shaped with many cell surface projections and were clumped together, overlapping with one another (*Figure 3I* and *J*). This abnormality was still obvious at E12.5 (*Figure 3K* and *L* and data not shown). Distal outflow tract septation had still not occurred in three of eight *RockDN;Wnt1-cre* embryos examined at E12.5 although it had occurred in all embryos examined at later stages. Thus, disrupted condensation of NCC was apparent in the outflow region from E10.5 and was associated with abnormal development of the intrapericardial arterial trunks.

Disturbance of Rock function can lead to detachment of cells from the matrix and cell death[14] and so we immuno-stained for cleaved caspase-3, a marker of apoptotic cells. However, although dying cells were abundant in the pharyngeal arches of mutant embryos,[15] there was little or no cell death within the outflow region of control or *RockDN;Wnt1-cre* mutants (Supplementary material online, *Figure S8*). In support of this, there was no significant differences between the overall numbers of NCCs in the aortic valve leaflets of mutant embryos compared with controls at E12.5 ($P = 0.37$; *Figure 3M*), suggesting that the abnormalities in valve structure were not due to NCC deficiency. However, there was a significant reduction in the number of NCCs in the non-coronary leaflet of the aortic valve in mutants compared with controls ($P < 0.005$; *Figure 3M*), suggesting that reduced contributions to this leaflet specifically might be relevant to abnormalities in valve leaflet patterning.

3.4 Roles for Rock in NC cell–cell adhesion and communication

We next wanted to examine how loss of Rock signalling in NCC affects the expression of factors known to be important in NCC behaviour in the outflow tract, as a way of better understanding why the valve patterning anomalies arise. Disruption of NCC aggregation and condensation suggested that there may be disturbance of intercellular adhesion and/or communication in NCC when Rock signalling was inhibited. As

Table 1 Arterial valve and coronary artery defects in *RockDN;Wnt1-cre* mutants at E15.5

	RockDN;Wnt1-cre mutants (%)	Controls
Aortic valve anomalies	27/31 (87)	0/30
Dysplastic bicuspid	13/31 (42)	0/30
Dysplastic quadricuspid	3/31 (10)	0/30
Dysplastic tricuspid	11/31 (35)	0/30
Pulmonary valve anomalies	26/31 (84)	0/30
Dysplastic bicuspid	3/31 (10)	0/30
Dysplastic quadricuspid	2/31 (6)	0/30
Dysplastic tricuspid	21/31 (68)	0/30
Ectopic coronary orifices	24/31 (77)	0/30
DORV	12/31 (39)	0/30
VSDs	12/31 (39)	0/30
SMC disorganization in aortic root	20/21 (95)	0/21
Disorganization of elastic laminae	7/21 (33)	0/21

Rock plays its key roles via effects on the cytoskeleton,[9] we examined both the actin cytoskeleton and cell junctional proteins in control and Rock-inhibited NCC. *In vivo* analysis was complemented by investigations using isolated NCC.

We first used a rhodamine–phalloidin conjugate to examine the actin cytoskeleton. Whereas the NCC contained within the outflow tract cushions of E10.5 control embryos exhibited abundant cortical stress fibres, these were reduced or missing from NCC within cushions of *RockDN* littermates (Supplementary material online, *Figure S9*). Phalloidin staining of the outflow tract myocardium was similar in both control and mutant sections, confirming the specificity of the effect for NCCs. Similarly, actin-based stress fibres were prominent in isolated control NCCs in culture, but were reduced in NCCs isolated from *RockDN;Wnt1-cre* embryos and isolated NCC treated with the Rock inhibitor Y27632 (Supplementary material online, *Figure S9* and data not shown).

The gap junction component connexin 43 (Cx43) is expressed in NCC,[19] localizing to points of contact between NCC migrating into the distal outflow tract in control embryos at E10.5, but this membrane localization was lost in NCCs within the distal outflow tract of *RockDN;Wnt1-cre* mutant embryos, with increased staining within the cytoplasm (*Figure 4A–D*). Although the levels of the cell–cell adhesion protein N-cadherin were too low to detect in NCCs within the outflow cushions at E10.5 and E11.5, despite being abundant in the outflow myocardium, β-catenin localized to the cell membrane in NCCs within the outflow tract cushions of control embryos (*Figure 4G* and *I*). In contrast, β-catenin was reduced in the membranes of NCCs within the outflow cushions of *RockDN* littermates (*Figure 4H* and *J*). *In vitro* analyses of Rock-inhibited NCCs confirmed these findings (*Figure 4E, F, K,* and *L* and Supplementary material online, *Figure S10*). Thus, these data suggest that cell–cell interactions, mediated by Rock, are essential for NCC aggregation and condensation within the outflow cushions.

3.5 NCC position the outflow cushions

We next asked why disruption of interactions between NCCs resulted in the bicuspid valves and outflow tract alignment defects seen in the mutant embryos. Serial sectioning of embryos was complemented by 3D reconstructions of the outflow region. For clarity, we refer to the distal, mid, and proximal regions of the outflow tract, as the appearance of the cushions varies along its length.

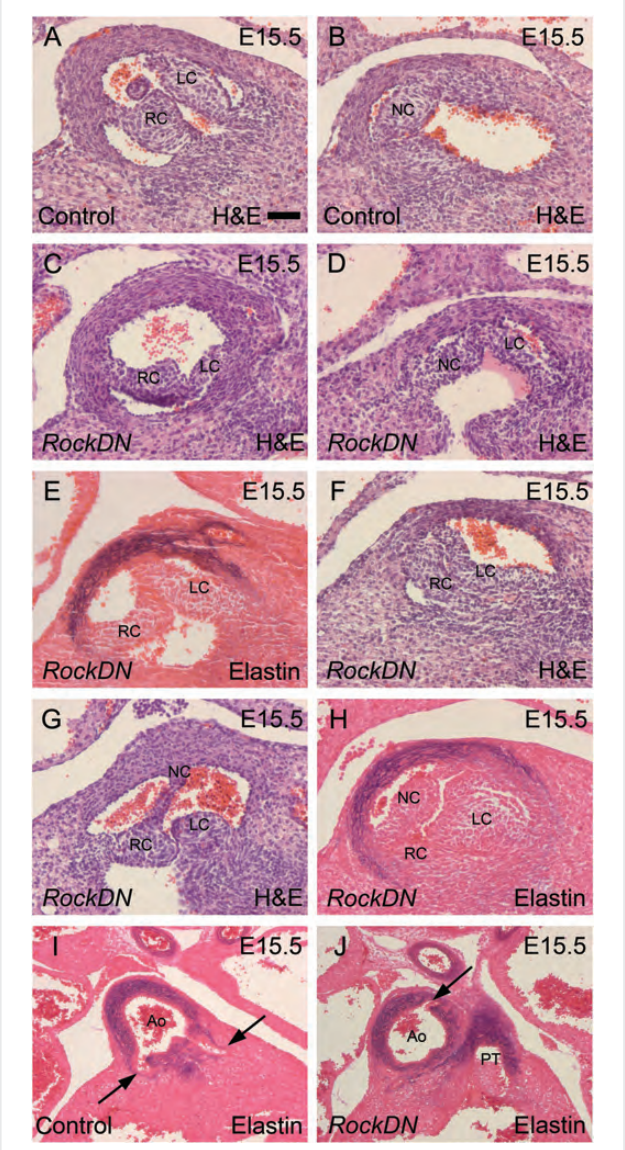

Figure 2 Arterial valve and coronary arterial anomalies in *RockDN;Wnt1-cre* mutants at E15.5. Sections are transverse. (*A* and *B*) The right and left coronary leaflets are seen together in one section of control aortic valves (*A*), while the non-coronary leaflet is seen in a more posterior section (*B*). (*C–H*) Bicuspid leaflets are seen in (*C–G*), whereas dysplastic but tricuspid leaflets are seen in mutants (*H*). (*I* and *J*) The coronary arteries derive from the right and left coronary sinuses in controls (arrows in *I*). An ectopic coronary artery, arising dorsally, is seen in mutant embryos (arrow in *J*). Ao, aorta; LC, left coronary; NC, non-coronary; PT, pulmonary trunk; RC, right coronary. Scale bar (*A–H*) = 50 μm, (*I* and *J*) = 100 μm.

The overall appearance of the outflow tract was similar in control and *RockDN;Wnt1-cre* embryos at E10.5, as NCC migrated into the outflow tract. In control embryos, the cardiac jelly was distributed evenly between the myocardium and endocardium along the length of the outflow tract (*Figure 5A* and *C* and Supplementary material online,

Figure S11). The NCCs were found throughout the circumference of the cardiac jelly in the most distal region (*Figure 5A*), whereas already in the mid-part, they were beginning to condense into superior and inferior clusters (*Figure 5C*); this altered the shape of the outflow lumen from a rounded to a more slit-like appearance. NCCs had not reached the most proximal outflow cushions at this stage (Supplementary material online, *Figure S11*). Thus, the separation of the NCC into superior and inferior clusters occurred before the appearance of discrete cushions. The NCCs were unevenly distributed around the circumference of the outflow tract in stage-matched *RockDN;Wnt1-cre* embryos at E10.5 (*Figure 5B* and *D*). Moreover, whereas NCC aggregated into superior and inferior clusters in the control embryo, this was not apparent in the mutant embryos and the lumen remained rounded (*Figure 5D*). Thus, whereas the precursors of discrete cushions were becoming apparent in E10.5 control embryos, this was not apparent in the *RockDN;Wnt1-cre* littermates.

By E11.5, two discrete cushions could be observed throughout the full length of the outflow tract in control embryos. These cushions, filled with NCC, were fused in the most distal region of the outflow tract (*Figure 5E*), but remained separated more proximally (*Figure 5G* and Supplementary material online, *Figure S4*). In contrast, the outflow cushions were unfused throughout the length of the outflow tract in four of five *RockDN;Wnt1-cre* embryos, and were malpositioned around the circumference in all five embryos examined (*Figure 5H*). NCC-filled cushion swellings could be observed but varied considerably from embryo to embryo. In some cases, these cushion swellings were hypoplastic (Supplementary material online, *Figure S4*), whereas in others they extended through the lateral region of the outflow tract, or more than two swellings could be seen (*Figure 5H* and Supplementary material online, *Figure S4*). Notably, additional 'cushions' always contained NCC. By E12.5, when septation of the outflow tract had occurred in all but its most proximal part, abnormal valve leaflets could be seen in the *RockDN;Wnt1-cre* embryos, with abnormal numbers and positioning of the leaflets (*Figure 5I* and *J* and Supplementary material online, *Figure S4I* and *J*). Thus, the forming cushions were abnormally patterned in the mutant embryos by E11.5, presaging the abnormal valve leaflets seen in mutant embryos by E12.5.

Three-dimensional reconstructions of the outflow cushions of control embryos at E11.5 showed that the two outflow cushions spiralled around one (Supplementary material online, *Figure S11*). In contrast, 3D views confirmed that the outflow cushions were malpositioned in *RockDN;Wnt1-cre* littermates. In the more extreme cases, cushion spiralling was much reduced with the tips of both cushions directed towards the right ventricle (Supplementary material online, *Figure S11F*), suggesting that these hearts would persist with both outlets connected to the right ventricle.

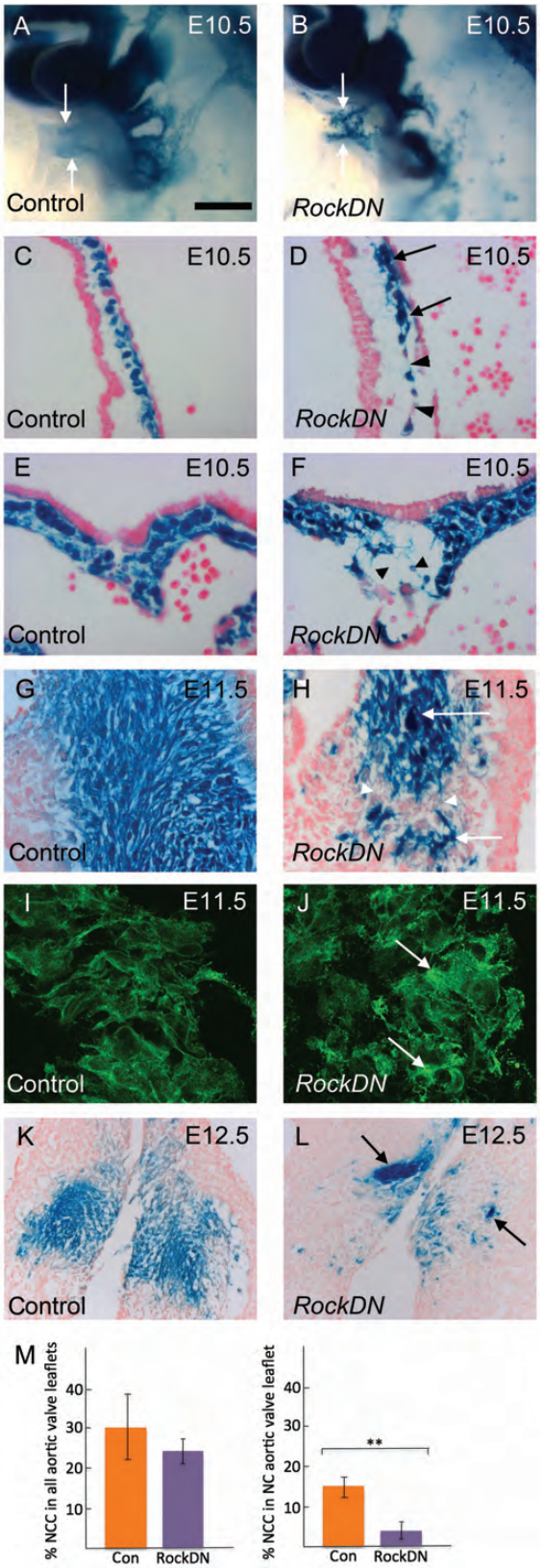

Figure 3 NCC defect in the developing outflow cushions. NCCs are blue in (*A*–*H*, *K*, and *L*) and green in (*I* and *J*). (*A*) and (*B*) are whole mounts, (*C*)–(*L*) are transverse sections. (*A* and *B*) NCCs appear disorganized in the outflow tract of the mutant (arrows). (*C*–*F*) NCCs are evenly distributed in control embryos in the outflow cushions (*C*) and the dorsal wall of the aortic sac (*E*). NCC clump, (arrows) or there are large spaces (arrowheads) between them, in mutant embryos (*D* and *F*). (*G*–*L*) NCCs condense in the outflow cushions at E11.5 in control embryos (*G*), but retain discrete cellular relationships (*I*). NCC clump (arrows), but are also abnormally separated (arrowheads), in stage-matched cushions of *RockDN;Wnt1-cre* embryos (*H*). Moreover, the NCCs are abnormally shaped and appear to overlap (*J*, arrows). This phenotype is maintained at E12.5 (*K* and *L*). (*M*) Quantification of NCC in the aortic valve leaflets of control and mutant embryos. Scale bar (*A* and *B*) = 80 μm, (*C*–*H*) = 50 μm, (*I* and *J*) = 25 μm, (*K* and *L*) = 100 μm. $^{**}P < 0.005$.

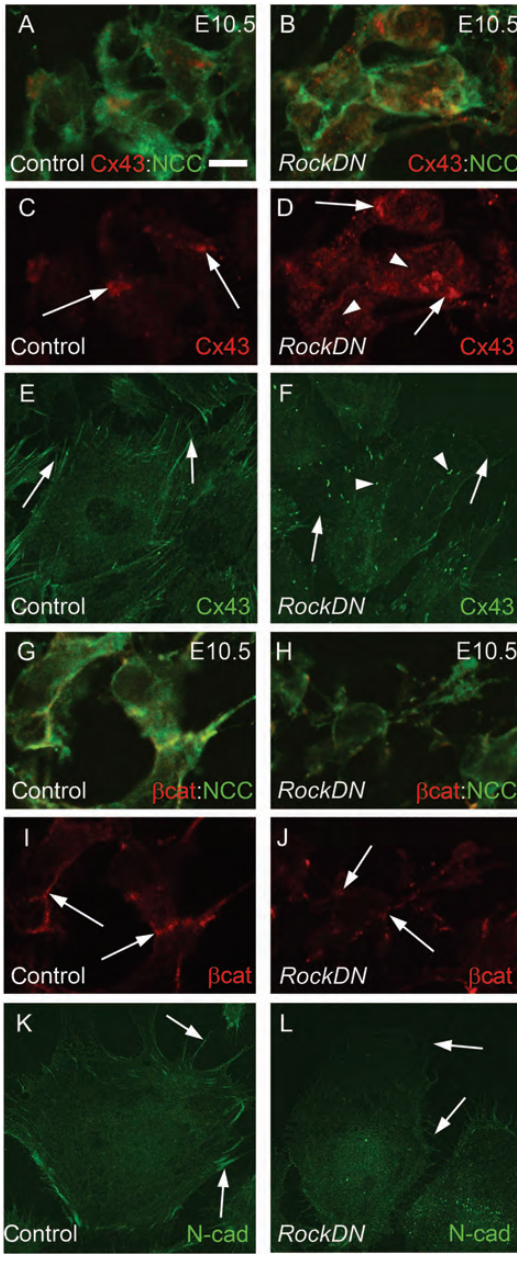

Figure 4 Abnormal cell–cell interactions in *RockDN;Wnt1-cre* NCC. (*A–D*) and (*G–J*) are from transverse sections and (*E*), (*F*), (*K*), and (*L*) are *in vitro* cultures. (*A–D*) At E10.5, Cx43 (red) is expressed at points of cell contact (arrows in *C*) between NCC (green) in the distal outflow tract. There is diffuse Cx43 expression within the cytoplasm of *RockDN;Wnt1-cre* NCC (arrows and arrowheads in *D*). (*E* and *F*) This is mirrored in control NCC *in vitro* where Cx43 is expressed at sites of contact with other NCC (*E*, arrows), whereas in cultures isolated from E9.5 *RockDN;Wnt1-cre* embryos, there is loss of staining between cells (arrows in F) and increased punctate staining within the cytoplasm (arrowheads in *F*). (*G–J*) β-catenin (red) is expressed uniformly (arrows in *I*) in cell membranes between neighbouring NCC in control outflow tract (green, *G*). In *RockDN;Wnt1-cre* embryos, β-catenin expression is reduced in the cell membrane and appears punctate (arrows in *J*). (*K* and *L*) N-cadherin is reduced in the cell membranes of isolated NCC from *RockDN;Wnt1-cre* embryos compared with controls (compare arrows *L* with *K*). β-cat, β-catenin, Cx43, connexin 43. Scale bar (*A–D* and *G–J*) = 5 μm, (*E*, *F*, *K*, *L*) = 15 μm.

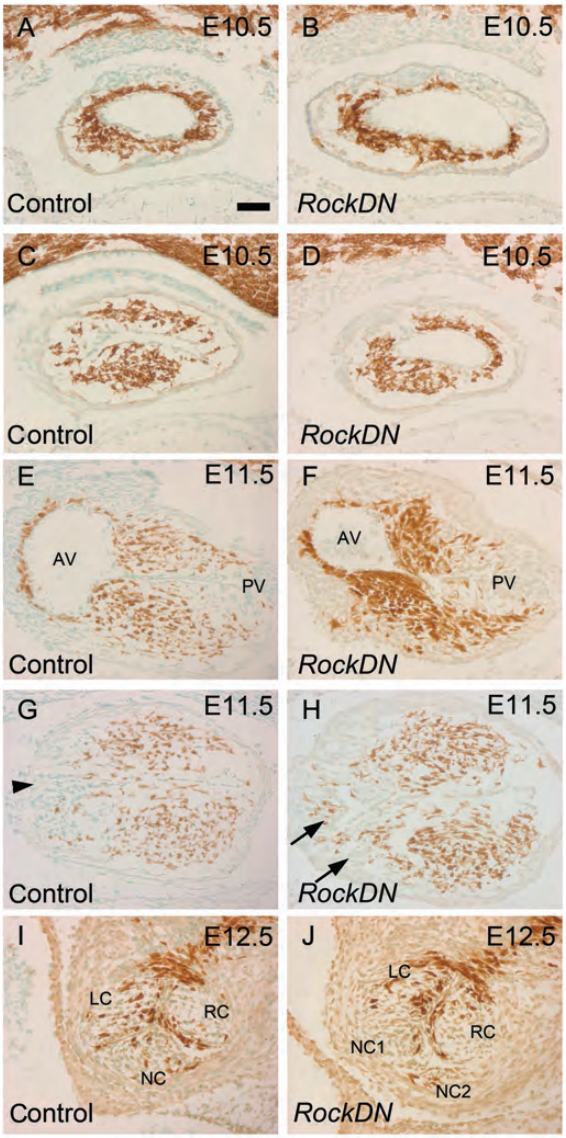

Figure 5 Abnormal positioning of the outflow cushions pre-figure arterial valve anomalies. All sections are coronal. NCCs are stained brown. (*A–D*) NCCs are found throughout the cardiac jelly in the distal outflow tract of control embryos at E10.5, although more proximally, in the mid-region (*C*), they have formed superior and inferior clusters and the lumen has a slit-like appearance. The NCCs are irregularly distributed in the mutant outflow (*B*). They remain circumferentially distributed in the mid-region and the lumen retains its rounded shape (*D*). (*E–H*) Fusion has occurred between the superior and inferior cushions at E11.5 in the distal region of the control outflow tract (*E*), whereas in the mid-region cushion apposition has not yet occurred although two large cushions and the aortic intercalated cushion (arrowhead in *G*) are apparent. The cushions appear relatively normal in the distal region of the mutant outflow (*F*). In the mid-region, the main cushions are irregularly sized and shaped and additional 'cushions', containing NCC, are apparent (arrows in *H*). (*I–J*) By E12.5, abnormally sized and patterned valve leaflets can be seen in *RockDN;Wnt1-cre* embryos. AV, aortic valve; PV, pulmonary valve; LC, left coronary; NC, non-coronary; RC, right coronary. Scale bar (*A–J*) = 50 μm.

4. Discussion

Although the link between dysmorphic arterial valves and degeneration of the walls of the aortic root is well established,[1] the underlying common mechanism remains poorly defined. Our studies suggest that the aggregation of NCC once they enter the outflow tract cushions affects where the discrete outflow cushions will form in the initially circumferential cardiac jelly that lines the initially solitary outflow tract. This likely acts together with other factors, including other cell types and haemodynamic effects of blood flow through the early unseptated heart, to define cushion position. The consequence of disrupting Rock signalling within NCCs is that well-defined, discrete, outflow cushions do not form, or are misplaced. In some cases the non-coronary leaflet does not form as a discrete entity and bicuspid valves appear to result. In other *RockDN;Wnt1-cre* hearts, the NCC clump together aberrantly producing additional 'cushions' that appear to presage quadriscuspid valves. Thus, our data suggest that the distribution of NCCs in the unseptated outflow tract predicts the pattern of valve leaflets formed after outflow septation (*Figure 6*). This is distinct from previous studies in the setting of NCC deficiency, which have suggested roles for NCC in valve remodelling in late gestation,[4] rather than early roles in valve leaflet patterning.

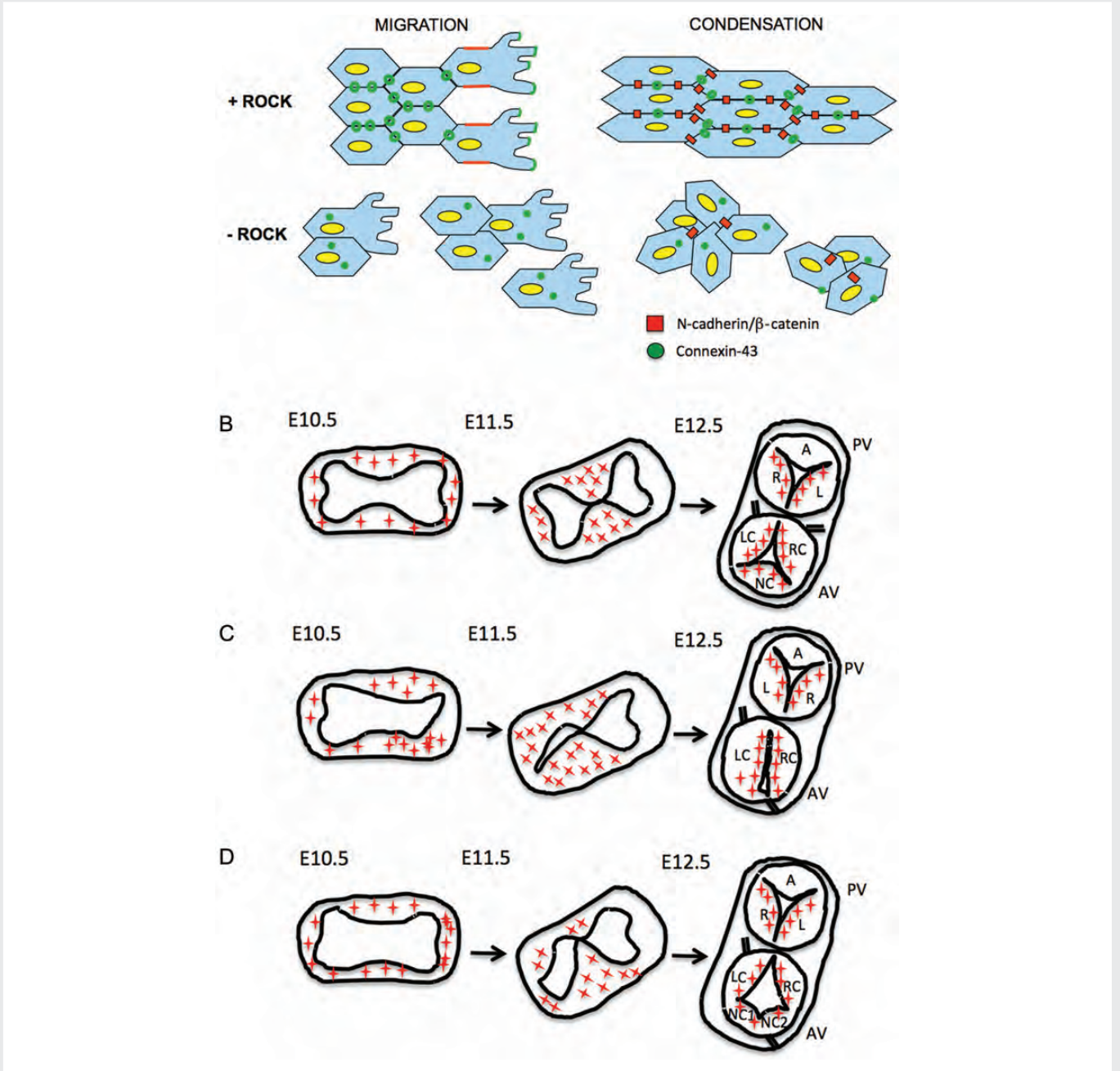

Figure 6 Model for abnormal arterial valve patterning. (*A*) Abnormalities in NCC adhesion and/or communication results in disrupted NCC condensation in the outflow cushions. (*B*) Distribution of NCC (red stars) in the mid-region of the outflow tract in control embryos as the outflow tract septates and the arterial valves form. (*C* and *D*) NCCs do not condense to pre-figure discrete cushions in *RockDN;Wnt1-cre* mutant embryos. As a consequence the valve leaflets are abnormally positioned and irregularly sized.

While cells derived from the endocardium and neural crest are known to make important contributions to the arterial valves,[4,20] the origins of the cells that form the non-adjacent leaflets are less clear. EDCs contribute to all leaflets of the arterial valves. However, whereas NCCs make major contributions to the right and left leaflets of both arterial valves, they make a reduced contribution to the non-coronary leaflet of the aortic valve, and almost no contribution to the anterior leaflet of the pulmonary valve. The relevance of this difference in embryonic origin of the cells that form the non-septal leaflets remains unclear. However, the greater contribution of NCCs to the non-coronary leaflet of the aortic valve may make it more susceptible to NCC disturbance, and explain the common occurrence of BAV; this is supported by the increased incidence of BAV compared with bicuspid pulmonary valve in our study. BAV has been reported in a number of mouse mutants, implicating Notch, eNOS, Gata5, and Alk2[4,21–24] in the development of the arterial valve leaflets. Studies in the Syrian hamster have implicated excessive fusion of the main outflow cushions in the aetiology of BAV,[25] although how this defect arises is unclear. The same authors suggested that abnormal outflow cushions led to the bicuspid valves in the eNOS null mouse,[26] but did not provide a cellular explanation. Thus, by showing that abnormal NCC aggregation leads to malpositioned outflow cushions, we provide what we believe to be the first cellular mechanism that explains how BAV can arise. Abnormal patterning of the coronary arteries was frequently found together with BAV in our study, as it is in humans.[27] As the valve patterning defects in the *RockDN;Wnt1-cre* mice appear to be attributable to abnormal cushion positioning, this suggests that cushion positioning may also determine where the coronary arteries connect with the valvar sinuses; this process is currently under investigation in our laboratory.

Correct positioning of the outflow cushions is also relevant to the aetiology of other outflow malformations. The reduced spiralling of the cushions in the mutant hearts likely contributes to the DORV, with failure of apposition of the proximal cushions to the ventricular septum explaining the persistent interventricular communication. BAV frequently occurs in combination with other NCC-associated abnormalities including coarctation of the aorta, persistent patency of the ductus arteriosus, abnormal positioning of the coronary ostia, and aortic wall anomalies.[1,3,4,27] Although we have been unable to establish whether *RockDN;Wnt1-cre* mutants develop coarctation of the aorta or persistent patency of the ductus arteriosus, as they die in the perinatal period before these anomalies become apparent, abnormalities in the wall of the aortic root, ascending aorta and pulmonary trunk, as well as ectopic positioning of the coronary ostia, are observed in the *RockDN;Wnt1-cre* mutant mice. Our data show that NCCs contribute to the wall of the aortic root and ascending aorta, and moreover, that SMCs are disrupted in these NCC-derived regions. We have shown previously that the outflow tract cushions, packed with NCC, form the adjacent parts of the aortic and pulmonary roots.[28] Thus, the abnormality in NCC condensation within the outflow cushions directly links the abnormalities in the NCC-derived SMC within the aortic and pulmonary roots with the abnormal patterning of the valve leaflets.

The observation that the NCCs lose contact with their neighbours, but also clump abnormally forming dense aggregates, can be explained if NCC communication is disrupted leading to randomized behaviour. We have shown that Rock is required for cell–cell adhesion and communication in NCCs within the outflow cushions. Rock is required for localization of N-cadherin to points of cell contact between NCC[29] and conditional deletion of N-cadherin from NCC resulted in loss of contact between neighbouring cells and outflow defects similar to those we observe.[30] Cx43, which is also lost from the cell surface in Rock-deficient NCC, has been implicated in communication between NCC.[19] Up-regulation of cell–cell adhesion proteins has been shown to be a feature of condensing cells,[31] thus, disruption of connexin 43, N-cadherin and/or β-catenin may be the cause of the abnormal NCC condensation in the outflow cushions (*Figure 6*). We conclude that abnormalities in cell–cell adhesion and communication can explain the abnormal cell behaviours and the outflow phenotypes that we observe when Rock function is attenuated. Moreover, we suggest that abnormalities in cushion positioning related to defects in these NCC aggregation processes may be a common mechanism that leads to BAV and associated anomalies.

Supplementary material

Supplementary material is available at *Cardiovascular Research* online.

Conflict of interest: none declared.

Funding

This work was supported by the British Heart Foundation (RG/07/007).

References

1. Siu SC, Silversides CK. Bicuspid aortic valve disease. *J Am Coll Cardiol* 2010;**55**:2789–2800.
2. Tadros TM, Klein MD, Shapira OM. Ascending aortic dilatation associated with bicuspid aortic valve: pathophysiology, molecular biology, and clinical implications. *Circulation* 2009;**119**:880–890.
3. Kappetein AP, Gittenberger-de Groot AC, Zwinderman AH, Rohmer J, Poelmann RE, Huysmans HA. The neural crest as a possible pathogenetic factor in coarctation of the aorta and bicuspid aortic valve. *J Thorac Cardiovasc Surg* 1991;**102**:830–836.
4. Jain R, Engleka KA, Rentschler SL, Manderfield LJ, Li L, Yuan L *et al*. Cardiac neural crest orchestrates remodeling and functional maturation of mouse semilunar valves. *J Clin Invest* 2011;**121**:422–430.
5. Kirby ML, Gale TF, Stewart DE. Neural crest cells contribute to normal aorticopulmonary septation. Science 1983;**220**:1059–1061.
6. Porras D, Brown CB. Temporal-spatial ablation of neural crest in the mouse results in cardiovascular defects. *Dev Dyn* 2008;**237**:153–162.
7. Vallejo-Illarramendi A, Zang K, Reichardt LF. Focal adhesion kinase is required for neural crest cell morphogenesis during mouse cardiovascular development. *J Clin Invest* 2009;**119**:2218–2230.
8. Nomura-Kitabayashi A, Phoon CK, Kishigami S, Rosenthal J, Yamauchi Y, Abe K *et al*. Outflow tract cushions perform a critical valve-like function in the early embryonic heart requiring BMPRIA-mediated signaling in cardiac neural crest. *Am J Physiol Heart Circ Physiol* 2009;**297**:H1617–H628.
9. Satoh K, Fukumoto Y, Shimokawa H. Rho-kinase: important new therapeutic target in cardiovascular diseases. *Am J Physiol Heart Circ Physiol* 2011;**301**:H287–H296.
10. Thumkeo D, Shimizu Y, Sakamoto S, Yamada S, Narumiya S. ROCK-I and ROCK-II cooperatively regulate closure of eyelid and ventral body wall in mouse embryo. *Genes Cells* 2005;**10**:825–834.
11. Thumkeo D, Keel J, Ishizaki T, Hirose M, Nonomura K, Oshima H *et al*. Targeted disruption of the mouse rho-associated kinase 2 gene results in intrauterine growth retardation and fetal death. *Mol Cell Biol* 2003;**23**:5043–5055.
12. Wei L, Roberts W, Wang L, Yamada M, Zhang S, Zhao Z *et al*. Rho kinases play an obligatory role in vertebrate embryonic organogenesis. *Development* 2001;**128**:2953–2962.
13. Groysman M, Shoval I, Kalcheim C. A negative modulatory role for rho and rho-associated kinase signaling in delamination of neural crest cells. *Neural Dev* 2008;**3**:27.
14. Kobayashi K, Takahashi M, Matsushita N, Miyazaki J, Koike M, Yaginuma H *et al*. Survival of developing motor neurons mediated by Rho GTPase signaling pathway through Rho-kinase. *J Neurosci* 2004;**24**:3480–3488.
15. Phillips HM, Papoutsi T, Soenen H, Ybot-Gonzalez P, Henderson DJ, Chaudhry B. Neural crest cell survival is dependent on Rho kinase and is required for development of the mid face in mouse embryos. *PLoS One* 2012;**7**:e37685.

16. Moase CE, Trasler DG. Delayed neural crest cell emigration from Sp and Spd mouse neural tube explants. *Teratology* 1990;**42**:171–182.
17. Soufan AT, Ruijter JM, van den Hoff MJB, de Boer PAJ, Hagoort J, Moorman AFM. Three-dimensional reconstruction of gene expression patterns during cardiac development. *Physiol Genomics* 2003;**13**:187–195.
18. Kramer TC. The partitioning of the truncus and conus and the formation of the membranous portion of the interventricular septum in the human heart. *Am J Anat* 1942; **71**:343–370.
19. Xu X, Francis R, Wei CJ, Linask KL, Lo CW. Connexin 43-mediated modulation of polarized cell movement and the directional migration of cardiac neural crest cells. *Development* 2006;**133**:3629–3639.
20. Jiang X, Rowitch DH, Soriano P, McMahon AP, Sucov HM. Fate of the mammalian cardiac neural crest. *Development* 2000;**127**:1607–1616.
21. Luna-Zurita L, Prados B, Grego-Bessa J, Luxán G, del Monte G, Benguría A *et al*. Integration of a Notch-dependent mesenchymal gene program and Bmp2-driven cell invasiveness regulates murine cardiac valve formation. *J Clin Invest* 2010;**120**:3493–3507.
22. Lee TC, Zhao YD, Courtman DW, Stewart DJ. Abnormal aortic valve development in mice lacking endothelial nitric oxide synthase. *Circulation* 2000;**101**:2345–2348.
23. Laforest B, Andelfinger G, Nemer M. Loss of Gata5 in mice leads to bicuspid aortic valve. *J Clin Invest* 2011;**121**:2876–2887.
24. Thomas PS, Sridurongrit S, Ruiz-Lozano P, Kaartinen V. Deficient signaling via Alk2 (Acvr1) leads to bicuspid aortic valve development. *PLoS One* 2012;**7**:e35539.
25. Sans-Coma V, Fernández B, Durán AC, Thiene G, Arqué JM, Muñoz-Chápuli R *et al*. Fusion of valve cushions as a key factor in the formation of congenital bicuspid aortic valves in Syrian hamsters. *Anat Rec* 1996;**244**:490–498.
26. Fernández B, Durán AC, Fernández-Gallego T, Fernández MC, Such M, Arqué JM *et al*. Bicuspid aortic valves with different spatial orientations of the leaflets are distinct etiological entities. *J Am Coll Cardiol* 2009;**54**:2312–2318.
27. Higgins CB, Wexler L. Reversal of dominance of the coronary arterial system in isolated aortic stenosis and bicuspid aortic valve. *Circulation* 1975;**52**:292–296.
28. Anderson RH, Chaudhry B, Mohun TJ, Bamforth SD, Hoyland D, Phillips HM *et al*. Normal and abnormal development of the intrapericardial arterial trunks in humans and mice. *Cardiovasc Res* 2012;**95**:108–115.
29. Comunale F, Causeret M, Favard C, Cau J, Taulet N, Charrasse S *et al*. Rac1 and RhoA GTPases have antagonistic functions during N-cadherin-dependent cell-cell contact formation in C2C12 myoblasts. *Biol Cell* 2007;**99**:503–517.
30. Luo Y, High FA, Epstein JA, Radice GL. N-cadherin is required for neural crest remodeling of the cardiac outflow tract. *Dev Biol* 2006;**299**:517–528.
31. DeLise AM, Tuan RS. Alterations in the spatiotemporal expression pattern and function of N-cadherin inhibit cellular condensation and chondrogenesis of limb mesenchymal cells *in vitro*. *J Cell Biochem* 2002;**87**:342–359.